FG.

AD A033498

⑥ STUDY OF NON-ISOENERGETIC TURBULENT JET MIXING IN A CONSTANT AREA DUCT.

⑨ Technical rept.,

⑩ J.H. Blasenak and W. Tabakoff

⑪ September 1976

⑫ 38 p.

D D C
DEC 20 1976
A

⑮

1423

038810 ✓

LB

Report No. 76-49

STUDY OF NON-ISOENERGETIC TURBULENT JET

MIXING IN A CONSTANT AREA DUCT

J.H. Blasenak and W. Tabakoff

September 1976

TABLE OF CONTENTS

ABSTRACT

A study of non-isoenergetic turbulent jet mixing between two streams has been conducted. Using a previously derived theoretical analysis for ducted mixing, an experimental investigation was performed to verify this theory and to determine the non-isoenergetic turbulent jet mixing characteristics in a constant area duct. Temperature profiles were measured at several axial locations in the duct for both a concentric and an eccentric configuration. It was determined that the theoretical and experimental temperature profiles agreed fairly well for both cases, although the concentric case showed better agreement than the eccentric case. It was also determined that a new constant of turbulence in the initial region was needed for non-isoenergetic mixing, mixing is generally more rapid than the theory predicted, the initial temperature difference between the two streams did not have much effect on the rate of mixing and a higher area ratio produced better agreement between the theory and the experimental data. It was concluded that the theory was good for a fairly simplified analysis.

NOMENCLATURE

Symbol

A	Cross sectional area of the duct, ft^2
AR	Area ratio
C	Experimental constant of turbulence (main region)
C_H	Experimental constant of turbulence (initial region)
c_p	Specific heat at constant pressure, Btu/lb °R
D	Diameter of the duct, ft
e	Eccentricity
$\bar{e}$	(e/R)
L	Length of the duct, ft
l	Nondimension length of the duct, (L/D)
M	Mach number
m	(Uh/Ul)
$\dot{m}$	Mass flow rate, lb/sec
n	Bypass ratio, $(\dot{m}_2/\dot{m}_1)$
P	Pressure
R	Radius of the duct, ft
r	Radial coordinate
r	Radius of the free jet
r_1	Radius of the primary ejector nozzle, ft
$\bar{r}$	(y/R)
T	Temperature, °R
T_t	Total temperature, °R
ΔT	$(T - T_2)$
U	Axial velocity component, ft/sec

ΔU $(U - U_h)$

X_k $\sqrt{\xi_k}$

x Axial coordinate

y Transverse coordinate

α Area ratio, (A_1/A_2)

β $(\phi/\phi-1)^{1/3}$

ϕ (Tm/T_2)

θ Temperature ratio, (T_2/T_1)

ρ Density, lb/ft^3

ξ (y/r)

ξ_k (R/r)

π 3.14159....

γ Ratio of specific heats

Subscripts

1   Primary stream

2   Secondary stream

3   Completely uniform mixed flow

h   Nominal wake conditions

m   At the axis

s   Static

w   Wall of the duct

1. INTRODUCTION

Previous analysis has shown that at medium and low flight
Mach numbers an exhaust gas jet of relatively small mass and
high velocity is an inefficient method of producing thrust.
This is due to the high energy losses at the nozzle exit and
the poor use of the kinetic energy of the exhaust jet for the
production of thrust. Two other important considerations for
current engines are good fuel economy and a low noise level.
In order to accomplish these objectives of maximizing thrust,
lowering fuel consumption and decreasing noise, a mixed flow
turbofan engine is the optimal candidate.

A high airflow is necessary to increase thrust while a
high jet velocity will increase thrust but decrease propulsive
efficiency. The turbofan engine produces a compromise between
maximum airflow and maximum jet exhaust velocity. Theoretical
studies have shown that the thrust of a turbofan engine can be
increased by mixing the hot primary jet with the colder
secondary airflow. Dr. Hartmann [1] confirmed these theories
with his experimental investigations at a bypass ratio of 3.2.
He reported a thrust gain, with equal total pressure in the
primary and secondary streams before mixing, for mixing
chamber inlet Mach numbers of 0.37 and below. The amount of
thrust gain was a function of the stream temperature and the
degree of mixing.

Therefore it is important to optimize the amount of mixing
in a turbofan nozzle. In order to optimize this mixing, it is
necessary to better understand the mechanics of turbulent jet
mixing. Although an actual turbofan engine may have turbine
exit swirl and an augmentor flame holder in the flow path, a
simplified analysis, which is both reliable and accurate, is
necessary before the more complex problem can be solved. To
satisfy this need for a tenable turbulent mixing theory, several
people have made analytical studies of mixing in recent years.
Several of these studies will be discussed in this paper. The
theory proposed by Khanna and Tabakoff [2], however, seemed to
provide a fairly simple yet promising approach to the turbulent
mixing problem. The theory lacked an experimental investigation
of the predicted results. Therefore, the current study was
performed to experimentally verify the accuracy of the theoretical
analysis of turbulent jet mixing between two concentric air
streams in a constant area duct. In particular the non-isoenergetic
(different stream temperatures) case was examined. An eccentric
mixing configuration was used as an additional experimental
study. Non-isoenergetic turbulent jet mixing experiments were
conducted, where the measured temperatures were compared with a
slightly modified version of Khanna and Tabakoff's theory. These
two non-isoenergetic mixing studies were believed to have
resulted in a better understanding of turbulent mixing in a
turbofan engine.

1

2. LITERATURE REVIEW OF RELATED THEORIES AND EXPERIMENTS

The main item which becomes apparent when doing a literature survey is the lack of information concerning turbulent ducted mixing for the non-isoenergetic case. The case of free turbulent mixing has been analyzed by many authors, such as Refs. [3], [4], [5], [6], [7], [8] and [9], and will not be reiterated here. The case of ducted isoenergetic turbulent mixing is examined in several works, such as Refs. [10], [11], [12], [13], [14], [15] and [16]. The best to date appears to be that of Razinsky [17]. The objective of his investigation was to determine the velocity field, the shear stress, and the pressure distribution from the well defined step change in the velocity profile at the mixing tube entrance to the limiting condition of fully developed flow. He integrates the equations of motion in the radial direction for preselected forms of the velocity profile. The assumptions used in this method are the mean radial velocity is small compared to the mean axial velocity, gradients in the axial direction are small relative to the radial gradients, and the viscous stress is small compared to the turbulent shear stress except near the wall. He performed an experimental investigation of his theory which generally produced good agreement between the theory and the experimental data. The inclusion of the wall boundary layer in the theoretical model yielded a significantly improved prediction of the pressure distribution compared to previous theories.

Of course the main reference for this paper, Ref. [2], considered both isoenergetic and non-isoenergetic turbulent mixing from an analytical viewpoint. An experimental investigation of the isoenergetic case was conducted in Ref. [18]. This study agreed with the theory of Ref. [2] for the case where the primary stream velocity was greater than the secondary stream velocity. In order to obtain this agreement, however, the coefficient of turbulence (c) had to be modified. Reference [2] used a value of c equal to 0.2. This value was recommended in Ref. [3]. It was experimentally determined for an axially symmetric free jet. For the case of confined jets, Ref. [18] experimentally determined a value of c equal to 0.7. The confining walls require the mixing to have this new constant of turbulence, which is completely different than that for the free jet case. In order to provide additional understanding of turbulent mixing an experimental investigation of eccentric isoenergetic ducted mixing was conducted in Ref. [19] and was compared with a slightly modified version of the theory of Ref. [2]. This work was expanded by the non-isoenergetic mixing experiments discussed in this paper.

3.   THEORETICAL ANALYSIS

Discussion

A review of the theoretical analysis described by Khanna and Tabakoff [2] is appropriate since it provided the basis upon which this study expanded. He found that, for free turbulent jets, the differential equations were favorable to an analytical solution and the experimental behavior was quite well known. Much less well known, however, was the behavior of a jet immersed in a secondary stream with confining walls present. Little experimental information on turbulent shear stress was available for jet flows other than free jets. Extensive measurements on free jets had shown that this type of flow was closely self-preserving, up to a certain distance downstream of the nozzle exit. Using the ideas of Abramovich [3] that hypothesized that the velocity or temperature profile in a duct would be the portion of a free jet profile located between the duct walls, he developed the following analysis for turbulent jet mixing between two subsonic streams in an axisymmetric constant area duct. His analysis included both the constant temperature (isoenergetic) mixing case and the different temperature for each stream (non-isoenergetic) mixing case.

Figure 1 illustrates the schematics of the ducted mixing system. It is divided into three flow regimes which are defined as follows:

1.   First regime or initial region. In this region turbulent mixing occurs between the secondary flow and the core of inviscid primary flow. When the inner boundary of this mixing region intersects with the axis of the jet, the region is ended.

2.   Second regime or transitional region. In this region the inviscid core of primary flow has been dissipated, but a region of inviscid secondary flow exists near the mixing chamber wall.

3.   Third regime or main region. In this region the mixing layer has spread to the wall and no portion of undisturbed secondary flow exists.

It is generally considered that the first and second regimes make up the initial region and that the third regime is considered the main region. The theory used here applies only to the main region. Other assumptions used by this theory are: viscous effects at the wall are negligible; the static pressure at any cross-section is constant; mixing obeys the perfect gas laws; and the duct walls are adiabatic.

Derivation of Equations

Since the general analytical problem is complex, the theory first addressed the isoenergetic case. Later the appropriate changes and additions were made for the non-isoenergetic case. The fundamental equations governing the flow in ducts are:

1. Conservation of Mass. For one-dimensional steady flow the continuity equation can be written as

$$\frac{\partial(\rho U)}{\partial x} = 0$$

or $\rho A U = \text{constant} = \dot{m}$

applying this equation to our model, we have

$$\rho_1 A_1 U_1 + \rho_2 A_2 U_2 = \rho_3 A_3 U_3 \tag{1}$$

2. Conservation of Momentum: Neglecting the viscous forces acting on the walls of the mixing chamber, we can write the momentum balance equation as

$$(p_3 - p_1)A_3 = \rho_1 U_1^2 A_1 + \rho_2 U_2^2 A_2 - \rho_3 U_3^2 A_3 \tag{2}$$

3. Conservation of Energy: Assuming the specific heat at constant pressure to be constant, independent of the temperature, the equation of conservation of energy is

$$\dot{m}_1 c_p T_{t_1} + \dot{m}_2 c_p T_{t_2} = \dot{m}_3 c_p T_{t_3} \tag{3}$$

4. Equation of State: For a perfect gas, the equation of state can be written as

$$p = \rho R T \tag{4}$$

Equations (1) to (4) determine the flow parameters after complete mixing, which occurs at an infinite distance from the initial cross-section of the mixing chamber. The calculations of flow parameters for a short mixing chamber, in which we have to take into account the incomplete mixing, and the determination of the optimum length of the mixing chamber, requires the knowledge of the laws of mixing for coflowing streams along the length of the mixing chamber.

4

In order to determine the variation of stream velocity and temperature along the radius of the mixing chamber at any cross-section, we shall make use of the hypothesis of universal ejection characteristics developed by Abramovich [3]. This hypothesis states that the nondimensional velocity and temperature profiles at any cross-section of a turbulent jet are universal functions of a parameter $\xi = (y/r)$, regardless of the external conditions of its development. In the ξ term, y is the distance from the axis in the transverse direction and r is the radius of the free jet. This hypothesis allows us to use the results of free-jet mixing theories to determine the velocity and temperature profiles for turbulent mixing of two streams in a duct. Mathematically, we can write the universal functions for nondimensional excess velocity and excess temperature profiles as:

$$\frac{\Delta U}{\Delta Um} = (1 - \xi^{1.5})^2 \tag{5}$$

$$\frac{\Delta T}{\Delta Tm} = (1 - \xi^{1.5}) \tag{6}$$

For axisymmetric turbulent mixing of free jets, $\xi = (y/r)$. But for mixing of two streams in a constant area mixing chamber, the maximum value of y is equal to R, the radius of the mixing chamber. The corresponding value of ξ is denoted by $\xi_k = (R/r)$, which is always less than one in the main region of the mixing chamber. Figure 2 better defines the terms used in these equations. This figure illustrates the basic concept used to find the velocity and temperature profile inside the duct. The excess velocity at the axis ΔUm, and the excess velocity ΔU, are defined by

$$\Delta Um = Um - Uh$$
$$\tag{7}$$
$$\Delta U = U - Uh$$

where   Um = axial velocity at the axis
      Uh = nominal wake velocity
      U = axial velocity at any value of y

The nominal wake velocity, Uh, can be obtained from Bernoulli's equation if it is assumed that the main change in the pressure occurs in the initial region, and that the longitudinal pressure gradient in the main region is small, i.e., a constant pressure is assumed for the whole main region. Therefore,

$$Uh^2 = U_2^2 - \frac{2}{\rho}(p_3 - p_2) \tag{8}$$

where p_3 is the pressure after completely uniform mixed flow has been attained.

5

Non-Isoenergetic Mixing

The analysis of the previous section will now be extended
to include the case of an initial temperature difference between
the two mixing airflows. This was the primary case of concern
to this author, since the purpose of the experiments was to
measure temperatures, to verify the theoretical analysis and to
predict the behavior of non-isoenergetic turbulent mixing in
a duct.

One can define a criterion for the degree of mixing as the
ratio of the total energy actually absorbed by the lower energy
stream to the maximum absorbable total energy, which corresponds
to perfect mixing of the streams with complete equalization of
states of the mixing gases. This essentially is a measure of the
degree of uniformity of the temperature profile in the mixing
duct. The variation of temperature along the radius of the mixing
duct at any cross-section will be determined by the universal
function of the parameter (ξ) as stated before. To determine
the variation of temperature along the length of the duct, we
shall write the integral relation which expresses the law of
conservation of mass as

$$\int_{0}^{A_3} \rho U \, dA = \rho_3 U_3 A_3 \tag{9}$$

Now adding and subtracting the quantity

$$\int_{0}^{A_3} \rho U h \, dA$$

from Equation (9), we have

$$\int_{0}^{A_3} \rho (U - Uh) \, dA + \int_{0}^{A_3} \rho U h \, dA = \rho_3 A_3 U_3 \tag{10}$$

Since

$$A_3 = \pi R^2$$

and

$$dA = 2\pi y \, dy$$

6

Therefore, Equation (10) becomes

$$2 \int_{0}^{R} \rho \Delta U y \, dy + 2Uh \int_{0}^{R} \rho y \, dy = \rho_3 U_3 R^2 \tag{11}$$

For approximately constant pressure mixing, using the equation of state, Equation (4), we have

$$\rho = \frac{p}{RT} \tag{12}$$

Substituting Equation (4) into (11), we have

$$2 \int_{0}^{\xi_k} (\Delta U/T) y \, dy + 2Uh \int_{0}^{\xi_k} (y/T) dy = U_3 R^2/T_3$$

Or

$$2 \int_{0}^{\xi_k} \frac{\Delta Um}{T} \frac{\Delta U}{\Delta Um} r^2 \frac{y}{r} d\left(\frac{y}{r}\right) + 2Uh \int_{0}^{\xi_k} \frac{y}{r} d\left(\frac{y}{r}\right)/T = \frac{u_3 R^2}{T_3} \tag{13}$$

Or

$$2 \Delta Um \int_{0}^{\xi_k} \left(\frac{\Delta U/\Delta Um}{T/Tm}\right) \xi d\xi + 2Uh \int_{0}^{\xi_k} \frac{\xi d\xi}{(T/Tm)} = u_3 \xi_k^2 (Tm/T_3) \tag{14}$$

Now $(\rho_1/\rho_2) = \theta = (T_2/T_1)$, $n = (\dot{m}_2/\dot{m}_1)$ and denoting $\phi = (Tm/T_2)$ we have

$$\frac{Tm}{T_3} = \frac{Tm}{T_2} \frac{T_2}{T_1} \frac{T_1}{T_3} = \phi \, \theta \, \left(\frac{n+1}{n\theta+1}\right) \tag{15}$$

Using Equation (6) and the expression for ϕ we have

$$(T/Tm) = \left[1 - \left(\frac{\phi-1}{\phi}\right) \xi^{1.5}\right] \tag{16}$$

Substituting Equation (16), (15) and (5) into Equation (14) we have

$$\frac{\Delta Um}{U_3} \int_{0}^{\xi_k} \frac{(1-\xi^{1.5})^2 \xi d\xi}{\frac{\phi}{\phi-1} - \xi^{1.5}} + \frac{Uh}{U_3} \int_{0}^{\xi_k} \frac{\xi d\xi}{\frac{\phi}{\phi-1} - \xi^{1.5}} = \frac{1}{2} \xi_k^2 \left(\frac{n+1}{n\theta+1}\right)\theta(\phi-1) \tag{17}$$

7

Integration of Equation (17) produces the following equation,

$$\frac{4}{A_1(\xi_k)} \left[\frac{\alpha(1+n\theta)-m(\alpha+1)}{\alpha\theta(n+1)}\right]\left[\frac{X_k^7}{7} + \frac{\beta^3-2}{4} X_k^4 - (\beta^3-1)^2\{X_k + \frac{\beta}{6} Z_1\right.$$

$$\left. + \frac{\beta\sqrt{3}}{18}\pi\}\right] + \frac{4m(\alpha+1)}{\alpha\theta(n+1)} [X_k + \frac{\beta}{6} Z_1 + \frac{\beta\sqrt{3}}{18}\pi] = \frac{X_k^4}{1-\beta^3} \qquad (18)$$

where:

$$X_k = \sqrt{\xi_k}$$

$$\beta = (\phi/\phi-1)^{1/3}$$

$$Z_1 = \ln \frac{(X_k - \beta)^2}{(X_k^2 + \beta X_k + \beta^2)} - 2\sqrt{3} \tan^{-1} (\frac{2X_k + \beta}{\beta\sqrt{3}})$$

$$A_1(\xi_k) = 1.0 - 1.143 \xi_k^{1.5} + 0.4 \xi_k^3$$

$$\alpha = (A_1/A_2)$$

$$m = (Uh/U_1) \qquad (19)$$

Equation (18) implicitly determines the quantity (Tm/T_2), where Tm is the temperature on the axis of the mixing duct at any cross-section. As can be seen from Equation (18), the quantity ϕ appears on both sides of the equation and therefore it is not possible to determine the temperature on the axis of the mixing duct for any specified location of the cross-section. Instead, a trial and error scheme is required to determine the temperature distribution along the length of the mixing duct. The details of the iterative scheme employed to solve Equation (18) on the CDC 6600 computer are given in Appendix A.

4.   TEST CONFIGURATION AND DESCRIPTION

Apparatus and Test Facilities

A.   Description of the test stand:

A schematic diagram of the mixing tunnel is shown in Figure 3. Air is supplied from an air pressure tank at 200 psia. The air passes through a pressure regulator in order to reduce the pressure of the flow to the desired value. As a rule, the pressure after the pressure regulator was held constant at 100 psia during each run, and was checked during the runs with the flow control panel.

8

The total air flow is measured with an orifice meter. The main flow is then divided into two flows, the primary and the secondary flows. The amount of mass flow in each is controlled with valves. The primary flow is routed through a pipe to the combustion chamber, which was used to heat the primary airflow. With the use of several different fuel flow nozzles and a fuel flow control panel, it was possible to regulate the primary flow temperature. The heated flow then passed through an insulated pipe until it arrived at the entrance to the mixing tunnel. The secondary air is measured with a second orifice meter, then it enters a settling chamber, in order to change its direction.

The primary flow passes through the settling chamber inside a two-inch diameter pipe which could easily be exchanged with another of diameter 1.4 inches. The primary flow pipe has a sharp edge so that the thickness at the initial mixing cross-section is practically zero. The secondary flow is then allowed to flow co-axially with the primary flow inside the mixing duct which extends five feet downstream. A movable rake was provided in the mixing duct. The mixing duct inside diameter was four inches.

The flow control panel is connected to pressure lines upstream of two orifice meters and is used to assure that the air pressure after the regulator is kept constant. A switch is connected to the flow control panel which could open the air line instantaneously.

B. Instrumentation

The air used during the test was supplied from a storage tank. During each run, the pressure inside the tank dropped continuously. If the pressure inside the tank began to drop below the pressure set up by the regulator, the mass flow of air began to change, and the conditions specified for a run changed. Therefore, the duration of the test was limited. In addition, it required between ten and twenty minutes to regulate and then stabilize the desired temperature of the primary flow. Monitoring of this temperature was also required during the run in order to maintain a constant temperature. Thus, it was essential to have a system of pressure and temperature probes that could quickly measure the radial distribution at each cross-section. Therefore, a temperature/pressure rake was built for the measurements.

A schematic drawing of the rake used is shown in Figure 4. Seven stainless steel tubes, each with an outside diameter of 0.13 inches, were connected to the rake. Five of the tubes were closed at the end with a copper-constantin thermocouple. The other two tubes were used to measure the total pressure. The tubes were equally spaced from each other at multiples of 0.5 inches from the duct centerline. Each pipe was secured at its proper distance inside the wedge-shaped rake. The rake shaft was installed to insure that it moved exactly along the mixing duct axis. The rake was connected to a shaft inside of which passed the pressure probes and thermocouple wires. They

9

ran from the rake to the appropriate data recorder instrument. The pressure probes were connected to a multi-tube manometer which also recorded the static pressure. The thermocouple wires were attached to a temperature recorder. This instrument converted the millivolt signals from the wires into the corresponding temperatures. These temperatures were then plotted on grid paper in a different color and number for each thermocouple. Thus, the temperatures could be read directly from the recorder in degrees Fahrenheit. The entire rake system slid along a scale so that an accurate position of the rake inside the mixing duct was known.

This test apparatus and instrumentation for the eccentric case was identical to the concentric case with the exception of the position of the primary flow tube. Both the 2.0 inch and the 1.4 inch diameter primary flow tubes were positioned inside of the 4.0 inch diameter duct in such a manner that their centerlines were displaced one-half inch below the duct centerline. In the concentric case the centerline was identical for both tubes. Figure 5 illustrates the eccentric configuration.

Testing Procedure and Accuracy

During each run the rake was set at a certain position and the multitube manometer was manually read. The temperature recorder worked automatically for the complete run. Readings were taken at only five axial locations due to the run time limitation. The five locations corresponded to five cross-sections located downstream of the initial mixing cross-section at distances of 0.2, 3, 5, 8, and 12 times the internal diameter of the mixing duct. This procedure permitted fairly quick measurements with a temperature error of approximately plus or minus five degrees Fahrenheit and a pressure error not greater than five percent for the case where the velocity was between 200 and 400 ft/sec.

The velocity was readily calculated from the formula

$$M^2 = \frac{2}{\gamma-1} \left[\left(\frac{P_T}{P_s}\right)^{\frac{\gamma-1}{\gamma}} - 1 \right] \tag{20}$$

Since both the total and static pressure and temperature at a given point were known.

Experimental Results

Three different test configurations were employed during the total experiment. These were: (1) Area Ratio = 3.0 and U1 > U2; (2) Area Ratio = 3.0 and U1 < U2; (3) Area Ratio = 7.16 and U1 > U2.

10

(A) Concentric Configuration - The experimental temperature profiles are plotted in Figure 6 for the Area Ratio = 3.0, U1/U2 = 2.4 and T1/T2 = 2.0 case at the five different cross-sections. Results for other temperature ratios can be found in Ref. [24]. A fully developed temperature profile was obtained for most of the results at an L/D equal to twelve (additional experimental results are given in Ref. [24]). This means that the nonuniformity of the temperature profile has disappeared due to the high degree of mixing in the duct. From the data obtained we find that the larger the initial temperature ratio, the longer it takes for the flow to become completely mixed. It was also observed that the temperature nonuniformity disappears more rapidly than the velocity nonuniformity. Velocity profiles were not plotted since they are given in Ref. [24].

Figure 7 is a plot of the experimental temperature profiles for the U1 > U2 case where the Area Ratio = 7.16. This area ratio was obtained by using a 1.4 inch diameter pipe inside the 4.0 inch diameter duct. Again the data taken at the five axial cross-sections is plotted. A fully developed temperature profile is again obtained at a distance equal to twelve times the diameter of the mixing duct (L/D = 12.0). The rate of decay of the temperature of the primary flow is higher than for the previous case where the area ratio was equal to three. In both the U1 greater than U2 cases, it was expected that the greater the velocity ratio or the temperature ratio, the greater the degree of turbulence, which would decrease the profile development length.

Figure 8 is a plot of the experimental temperature profiles for the U1 less than U2 case where the area ratio equals 3.0, the velocity ratio is 0.59 and the temperature ratio is 1.65. The data shows that the final temperature is heavily influenced by the secondary stream temperature. This is due to the fact the bypass ratio is high and the primary flow is rapidly damped out. The low temperature ratios indicated more rapid mixing in the U1 greater than U2 cases, and this is also true for the U1 less than U2 case.

(B) Eccentric Configuration - The first case is again the U1 greater than U2 configuration at an area ratio equal to 3.0. Figure 9 represents the experimental temperature profiles at the five axial locations along the duct which were measured for this case. Figure 10 shows a configuration where U1 is greater than U2, but the area ratio is equal to 7.16. The temperature and velocity ratio values are a repeat of the same values used for concentric mixing. Figure 11 represents the U1 less than U2 configuration at an area ratio of 3.0. The same velocity ratios as the concentric experiments were used.

From the temperature curves presented in Figures 9, 10 and 11 it is apparent that the temperature profiles are always un-symmetrical about the axis of the mixing duct. At the cross-

sections near the initial cross-section, the maximum temperature is at the axis of the primary flow. But as one proceeds downstream the peak temperature tends to move toward the wall on the side of the eccentricity. Additionally, the temperature non-uniformity does not decay with the same rate as in the case of concentric mixing. The temperature decays more rapidly with increasing area ratio and when U1 is less than U2, this agrees with the expected result. All three configurations behave in the same general fashion with regard to temperature profile decay. The profile remains unsymmetrical even at the final cross-section measured (i.e., L/D = 12.0). It is seen that eccentricity increases the axial distance required for a fully developed profile to be obtained. The rate of decay of the temperature profile does not appear to have a direct relationship to either the primary temperature magnitude or the temperature ratio. The rate of decay appears to be fairly consistent with respect to these variables. This is again different than the velocity mixing studies, where the rate of decay of the velocity at the primary flow axis increased with both increasing velocity ratio and velocity magnitude.

5. RESULTS AND DISCUSSION

A preliminary examination of the test data indicated that the temperature mixing was much more rapid than the theory predicted. Therefore, based on the experience of Ref. [18] where a new value of the constant of turbulence (c) for the main region was experimentally obtained, a computer check was made on other values of c. It was found that increasing the value of c, even to a value of 20, did not significantly improve the agreement between the theoretical and experimental data. Another approach was deemed necessary. Following the background and reasoning of Ref. [18], the values of the temperature at the axis (Tm) and the temperature near the wall outside the boundary layer (Tw) were plotted for various values of L/D along the mixing duct. Instead of changing the value of c, however, the value of c_H, the constant of turbulence in the

initial region, was varied and the resulting theoretical values of Tm and Tw were plotted. Since it was apparent that the initial temperature difference of the two streams caused the mixing to be accelerated, it was reasonable to assume that the accelerated mixing would also affect the mixing in the initial region and hence shorten the axial length of the initial region. Various values of c_H were plotted against the experimental data in Figure 12. A value of $c_H = 0.36$ presented the best agreement between the theory and the experimental data. The case where U1 was less than U2 was not considered significant due to the negative results of [18] and an examination of our experimental test results, which showed that good agreement was not obtained.

With the value of $c_H = 0.36$ and the value of c = 0.7 the computer program was run to obtain the theoretical curves used

12

to compare with the experimental data.

After having examined the experimental temperature profile plots and the theoretical versus experimental temperature plots, several observations can be made. The accuracy of the temperature measurement system should be kept in mind when comparing various temperature values. Within these restraints the data agrees reasonably well with the experiments for the cases where U1 is greater than U2. There can be seen a definite trend for the experimental data to have a lower temperature than the theoretical data at higher L/D values. The cause of this observed phenomenon is believed to be the fact that heat loss occurred through the duct walls during the tests. Thus the adiabatic wall assumption is probably not valid for these experiments. This phenomenon will be examined further in the subsequent sections.

Theoretical versus Experimental mixing comparison for the concentric case - As was previously discussed, a new value of the constant of turbulence for the initial region was required to account for the increased degree of mixing which was exhibited by the experimental data. This new value helped in the agreement of the theoretical and experimental data for the cases where U1 was greater than U2. It did not help in the U1 less than U2 cases. Using the new value of the constant of turbulence (Ch = 0.36) a comparison between theory and experiment was made with plots for the following cases. It should be noted that T1 is greater than T2 for all mixing cases.

Case I: U1 > U2, Area Ratio = 3.0

Figure 13 illustrates this case for velocity ratio of 2.4 approximately. Each curve on the figure represents a temperature profile at the given cross-section for different values of temperature ratio. The rapid degree of the disappearance of the initial temperature nonuniformity is readily apparent. At large values of L/D (Ref. [24]), the experimental temperature profile has a lower mean temperature than the theoretical temperature profile. This phenomenon was due to the heat loss through the wall of the duct. In general, the agreement between theory and experiment is fairly good. The velocity ratio does not seem to have much effect on the degree of mixing within the accuracy limits of the data. As was previously mentioned the temperature profile becomes fully developed more quickly for a lower temperature ratio.

Case II: U1 > U2, Area Ratio = 7.16

This case is illustrated by Figure 14. Again a plot is made for a given velocity ratio and a given L/D with curves of two different temperature ratios. Because of the higher area ratio, the initial region length is decreased. Case II figure

13

shows a lesser effect of heat loss. Only a small decrease in the experimental temperature data is seen at an L/D equal to twelve (Ref. [24]). This is the expected result since the mass flow of cold secondary air compared to the mass flow of hot primary air is significantly larger than for Case I. The lower average temperature in the partially mixed flow contributes to much less heat loss through the duct wall. The agreement between the Case II experimental and theoretical temperature profiles is quite good.

6. CONCLUSIONS

An experimental investigation of non-isoenergetic turbulent jet mixing between two streams in an axisymmetric duct has been conducted. Experimental temperature profiles have been measured at several axial locations in the duct. They have been compared with the theoretical temperature profiles determined by the analysis described in this paper. Several conclusions can be made from these comparisons.

It was determined that the theory and experimental results agree fairly well for the concentric case where the primary stream velocity is greater than the secondary stream velocity. This is true for both area ratios tested. The velocity ratio had no significant effect on the rate of temperature mixing of the flow. Also, contrary to the theory, the mixing process was not accelerated by a larger initial temperature difference between the flows. The opposite effect appeared to be the actual effect. It was experimentally verified, however, that energy diffuses more rapidly than momentum. The rate of mixing determined by the concentric mixing experiments indicated that the mixing was more rapid than the theoretical analysis had predicted.

The theory used in this analysis is a fairly simple one which produces reasonably good results. Eliminating a couple of the simplifying assumptions would provide better agreement with the experimental data. However, it is not thought that the increased complexity is worth the additional effort.

REFERENCES

1. Hartmann, Ing. A., "Theoretical and Experimental Investigation on Fan-Engines with Mixing: Optimal Layout of Fan-Engines with and without Mixing," AIAA 3rd Propulsion Joint Specialists Conference, July 1967, Paper 416.

2. Khanna, K.K. and Tabakoff, W., "A Study of Non-Isoenergetic Turbulent Jet Mixing Between Compressible Subsonic Streams in Axisymmetric Constant Area Duct," Project Themis Report No. 69-1, University of Cincinnati, August 1969.

3. Abramovich, G.N., "The Theory of Turbulent Jets," MIT Press, Cambridge Mass., 1963.

4. Alpinieri, Louis, "Turbulent Mixing of Co-axial Jets," AIAA Journal, Vol. 2, No. 9, Sept. 1964.

5. Maise, G. and McDonald, H., "Mixing Length and Kinematic Eddy Viscosity in a Compressible Boundary Layer," AIAA Journal, Vol. 6, No. 1, January 1968.

6. Hinze, J., "Turbulence, An Introduction to its Mechanism and Theory," McGraw Hill Book Co., 1959.

7. Bradshaw, P., Ferriss, D., and Atwell, N., "Calculation of Boundary Layer Development Using the Turbulent Energy Equation," Journal of Fluid Mech., Vol. 28, Part 3, 1967, pp. 593-616.

8. Zawacki, T. and Weinstein, H., "Experimental Investigation of Turbulence in the Mixing Region Between Coaxial Streams," NASA Contractor Report, CR-959, February 1968.

9. Ortwerth, P., "Mechanism of Mixing of Two Non-reacting Gases," AFAPL-TR-71-18, October 1971.

10. Edelman, R. and Fortune, O., "An Analysis of Mixing and Combustion in Ducted Flows," AIAA Paper No. 68-114, Jan. 1968.

11. Hill, Philip, "Turbulent Jets in Ducted Streams," Journal Fluid Mech., Vol. 22, Part 1, 1965, pp. 161-186.

12. Drewry, J., "Supersonic Mixing and Combustion of Confined Coaxial Hydrogen-Air Streams," AIAA Paper No. 72-1178, December 1972.

13. Hendricks, C. and Brighton, J., "Prediction of Swirl and Inlet Turbulence Kinetic Energy Effects on Confined Jet Mixing," ASME Paper No. 75-FE-2, January 1975.

14. Hedges, K. and Hill, P., "Compressible Flow Ejectors, Part I," ASME Paper No. 74-FE-1, February 1974.

15. Hedges, K. and Hill, P., "Compressible Flow Ejectors, Part II," ASME Paper No. 74-FE-2, February 1974.

16. Burley, R. and Bryant, L., "Experimental Investigations of Coaxial Jet Mixing of Two Subsonic Streams at Various Temperature, Mach Number, and Diameter Ratios for Three Configurations," NASA MEMO 12-21-58E, February 1959.

17. Razinsky, E., "Turbulent Mixing of Confined Axisymmetric Jets," University Microfilms, Ann Arbor, Michigan, 1969.

18. Tabakoff, W. and Hosny, W., "Theoretical and Experimental Investigations on the Mixing of Isoenergetic Confined Coaxial Jets," Project Themis Report No. 70-10, University of Cincinnati, June 1970.

19. Tabakoff, W. and Hosny, W., "Theoretical and Experimental Jet Mixing of an Eccentric Primary Jet in a Constant Area Duct," Project Themis Report No. 70-11, University of Cincinnati, July 1970.

20. Harsha, P.T., "Prediction of Free Turbulent Mixing Using a Turbulent Kinetic Energy Method," Langley Working Conference on Free Turbulent Shear Flows, NASA Langley Research Center, July 1972.

21. Harsha, P.T., "Free Turbulent Mixing: A Critical Evaluation of Theory and Experiment," AEDC TR 71-36, February 1971.

22. Harsha, P.T. and Lee, S.C., "Analysis of Coaxial Free Mixing Using the Turbulent Kinetic Energy Method," AIAA Journal, Vol. 9, No. 10, October 1971, pp. 2063-2066.

23. Lee, S.C. and Harsha, P.T., "Use of Turbulent Kinetic Energy in Free Mixing Studies," AIAA Journal, Vol. 8, No. 6, June 1970, pp. 1026-1032.

24. Blasenak, J.H., "An Experimental Investigation of Non-isoenergetic Turbulent Jet Mixing in a Constant Area Duct," M.S. Thesis, University of Cincinnati, 1976.
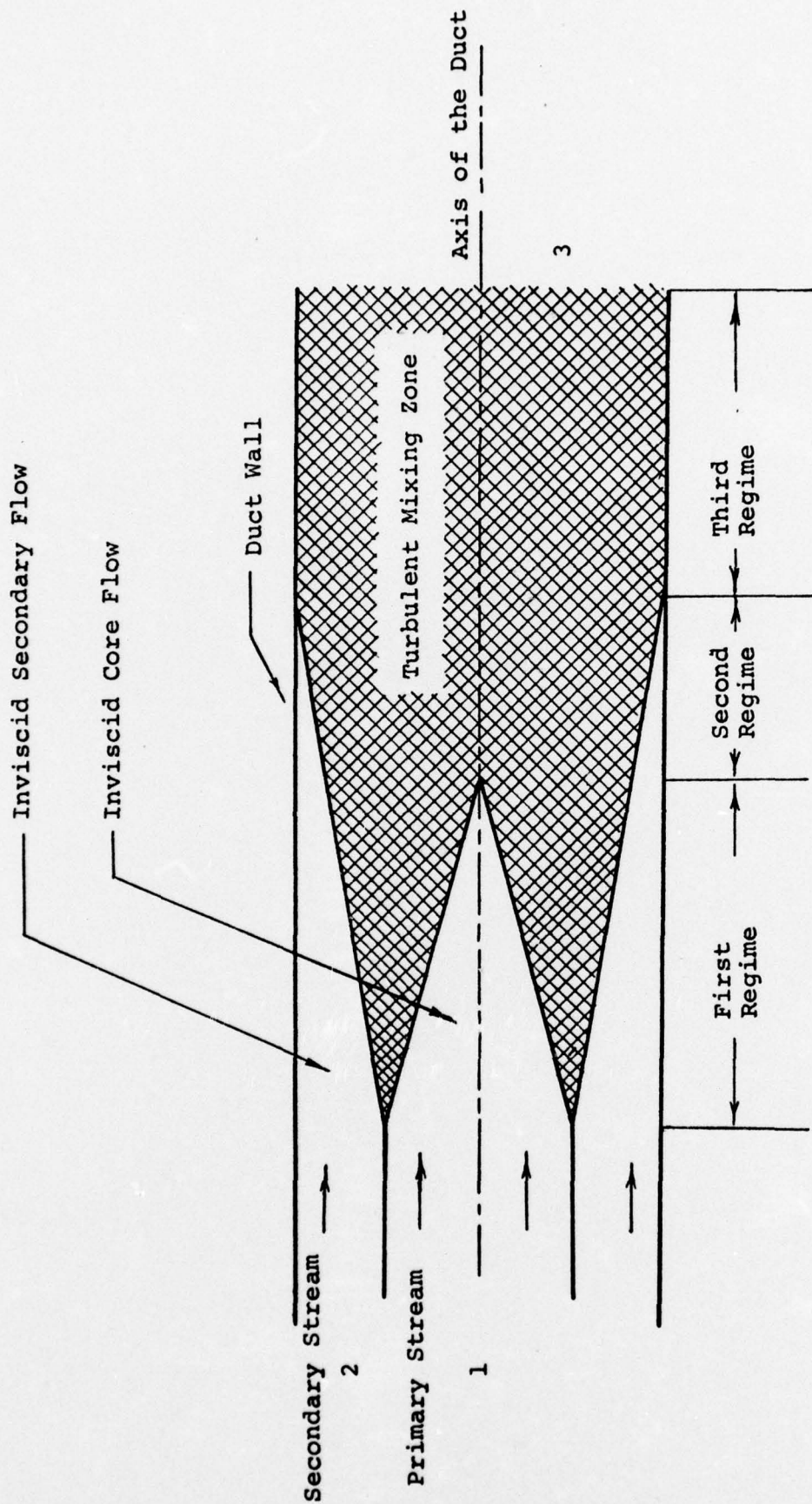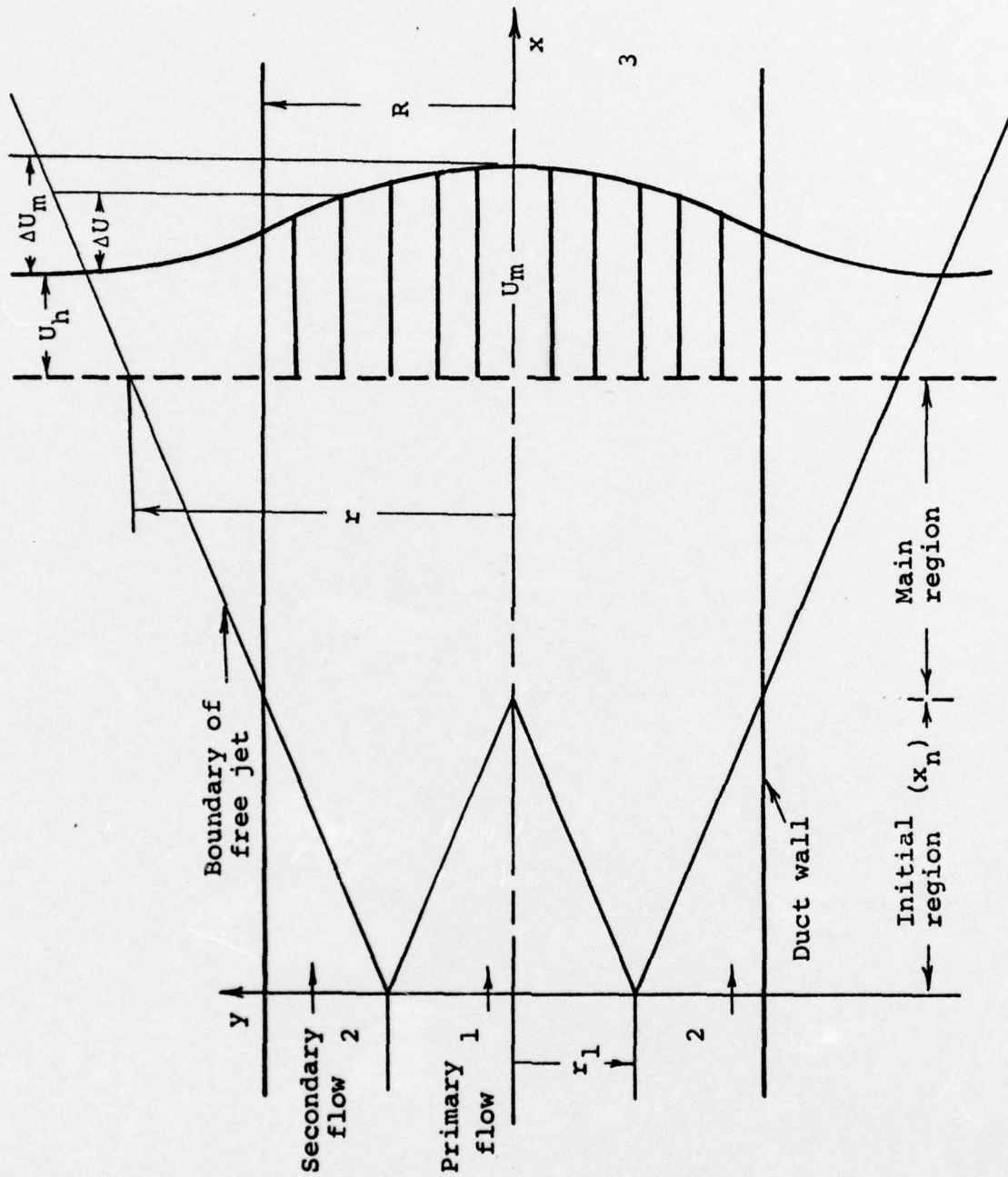
FIGURE 1   Schematic of Ducted Mixing System

17

FIGURE 2   Schematic Diagram of Confined Jet Mixing
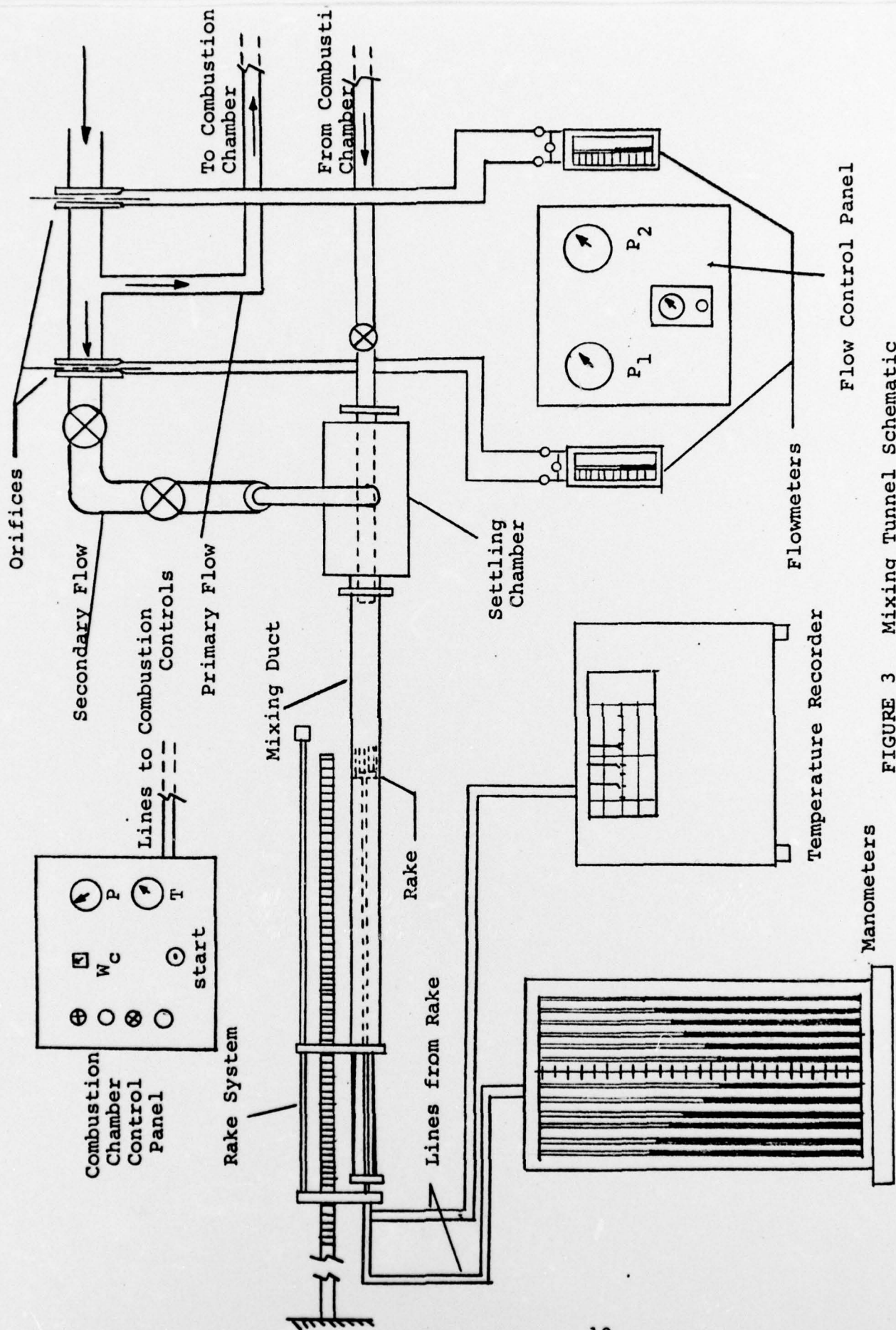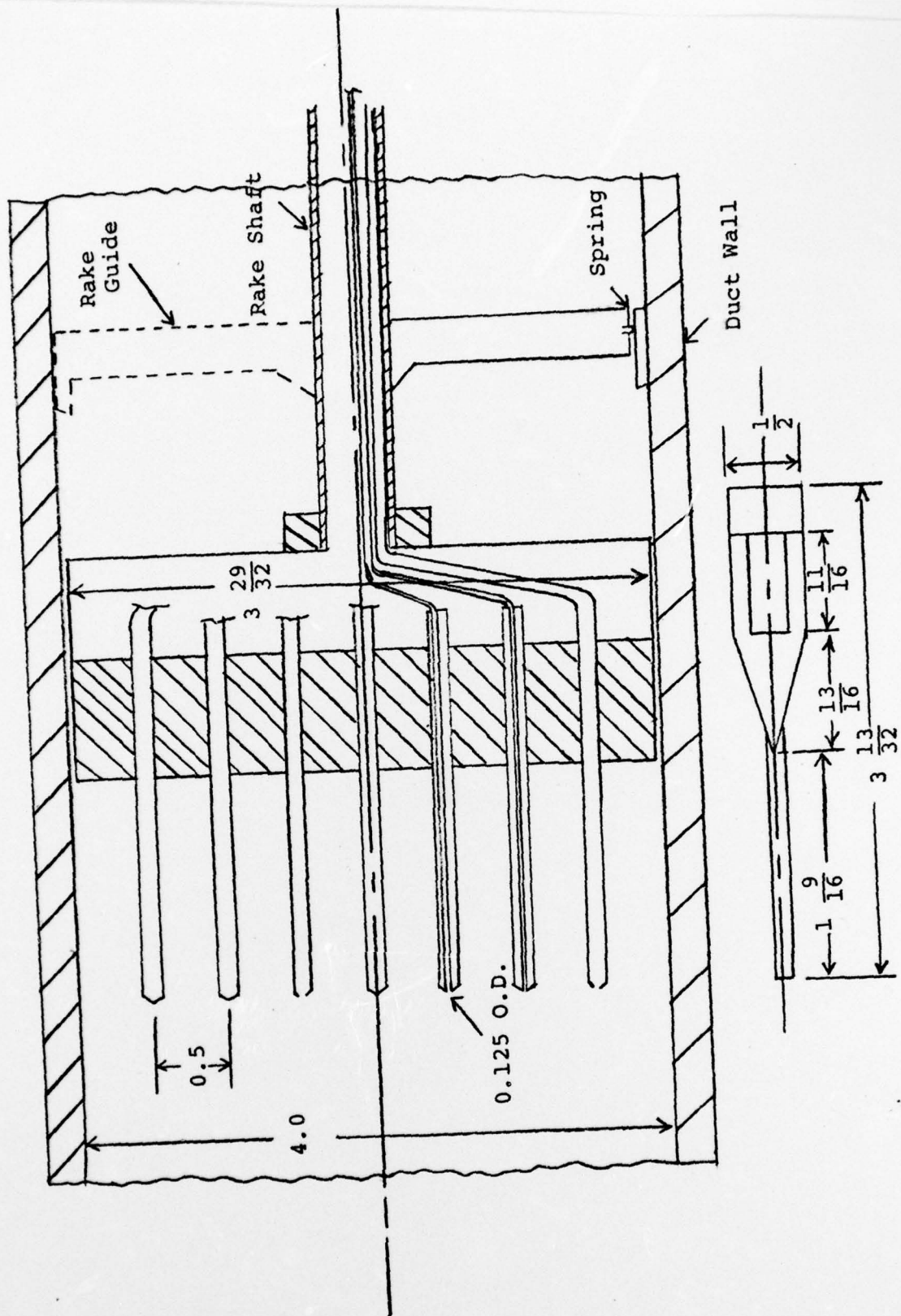
18

FIGURE 3   Mixing Tunnel Schematic
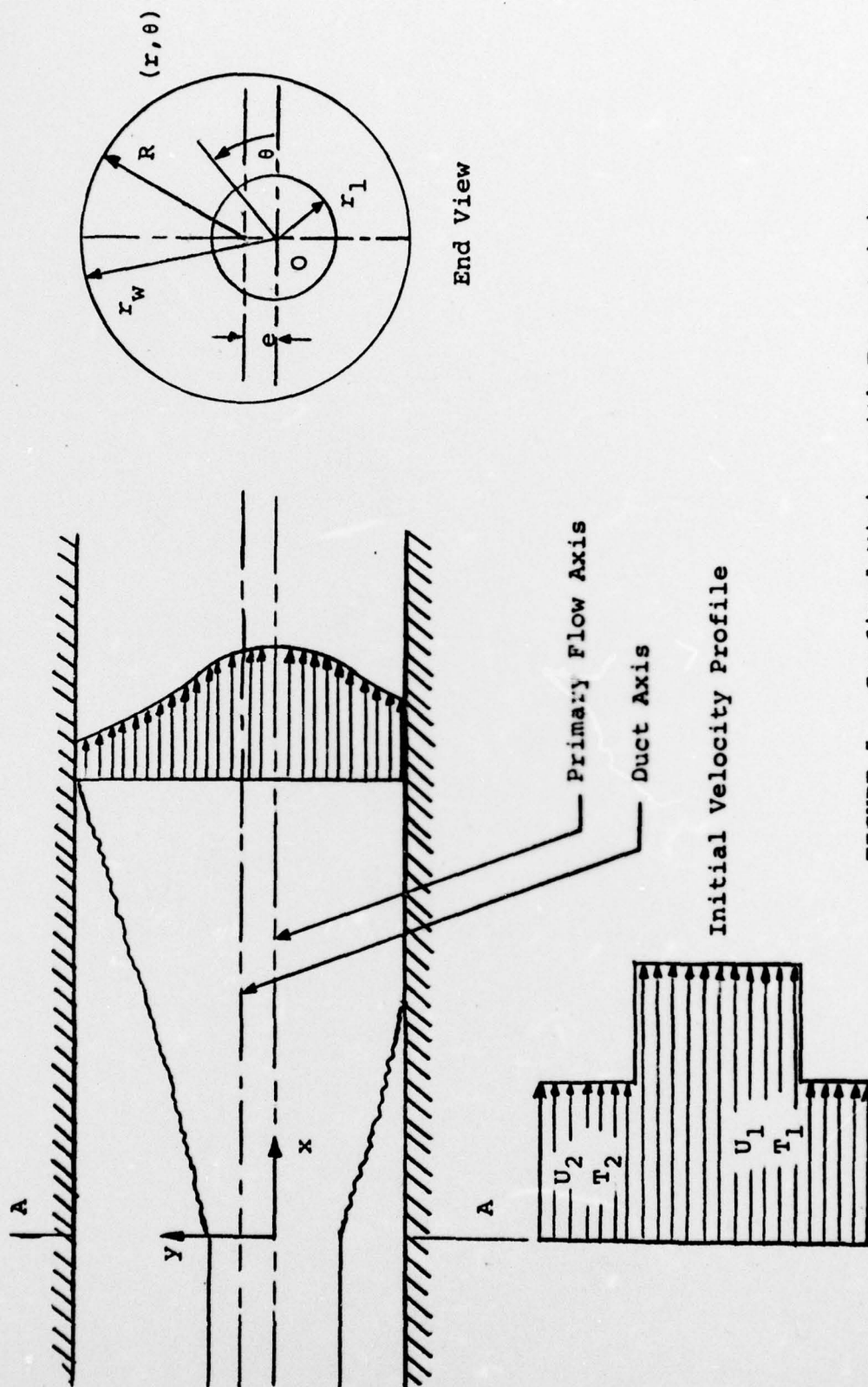
FIGURE 4   Temperature/Pressure Rake

FIGURE 5   Confined Mixing with Eccentricity

EXPERIMENTAL TEMPERATURE PROFILES
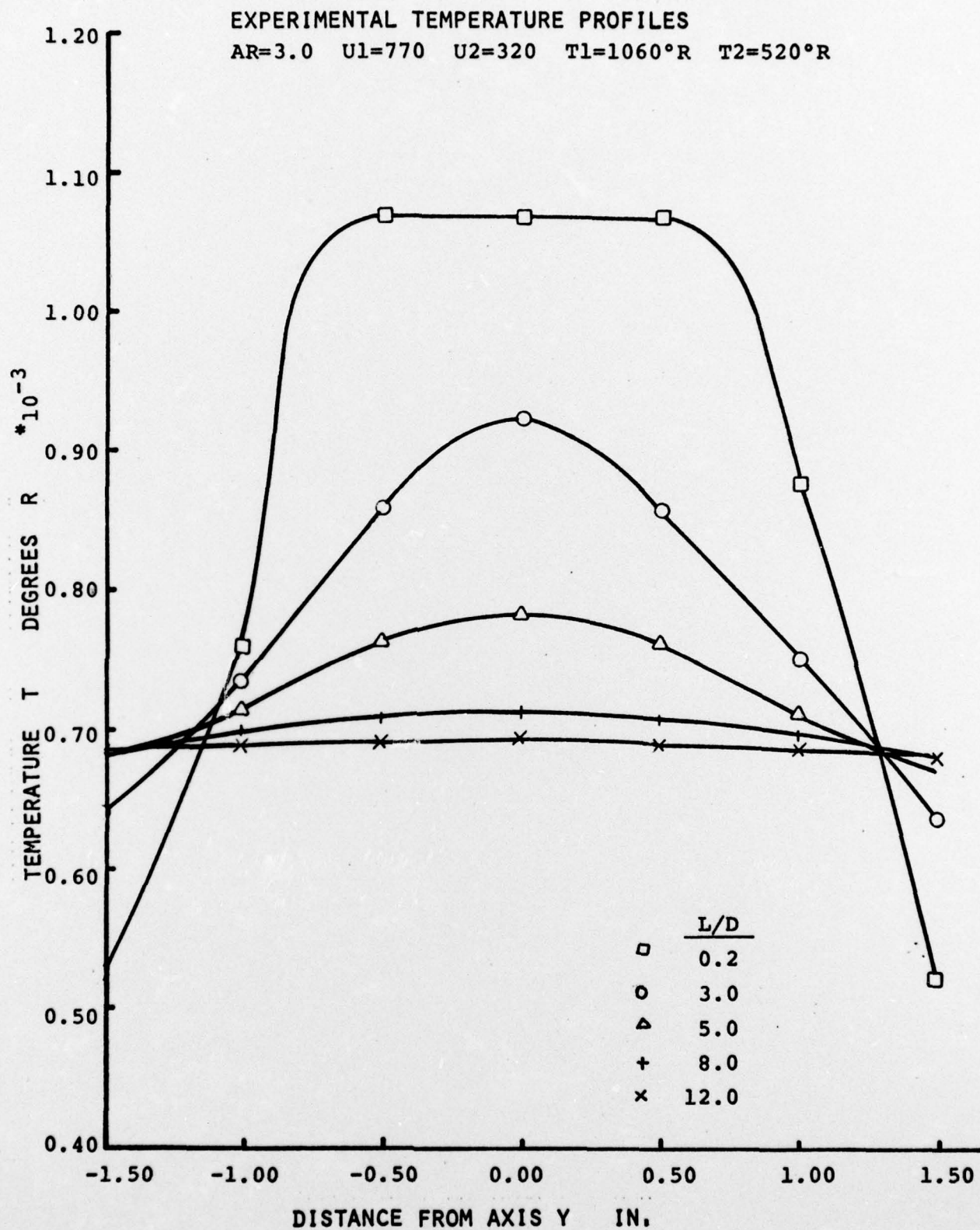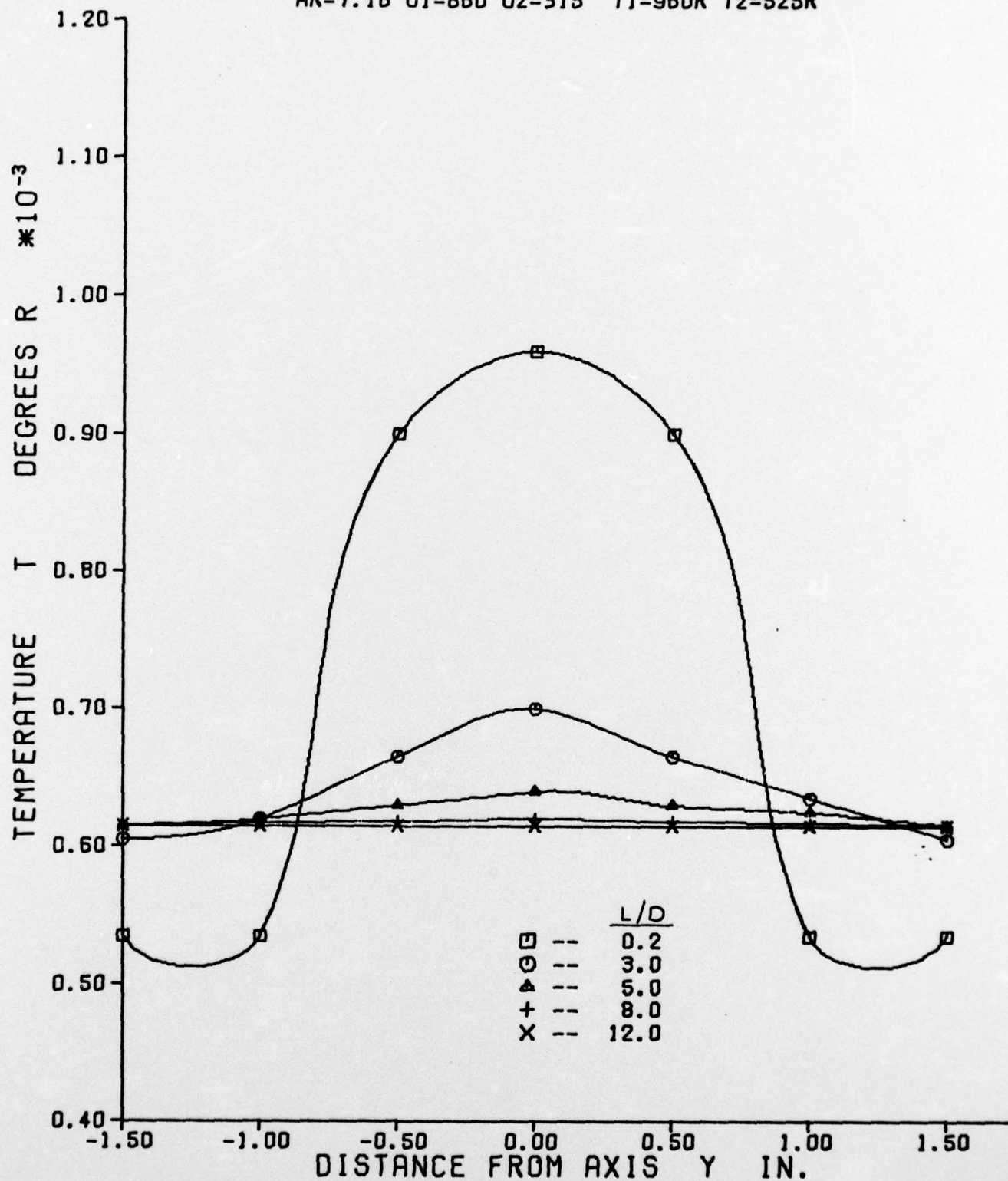AR=3.0   U1=770   U2=320   T1=1060°R   T2=520°R

FIGURE 6

EXPERIMENTAL TEMPERATURE PROFILES
AR=7.16 U1=860 U2=315 T1=960R T2=525R

FIGURE 7

23

EXPERIMENTAL TEMPERATURE PROFILES
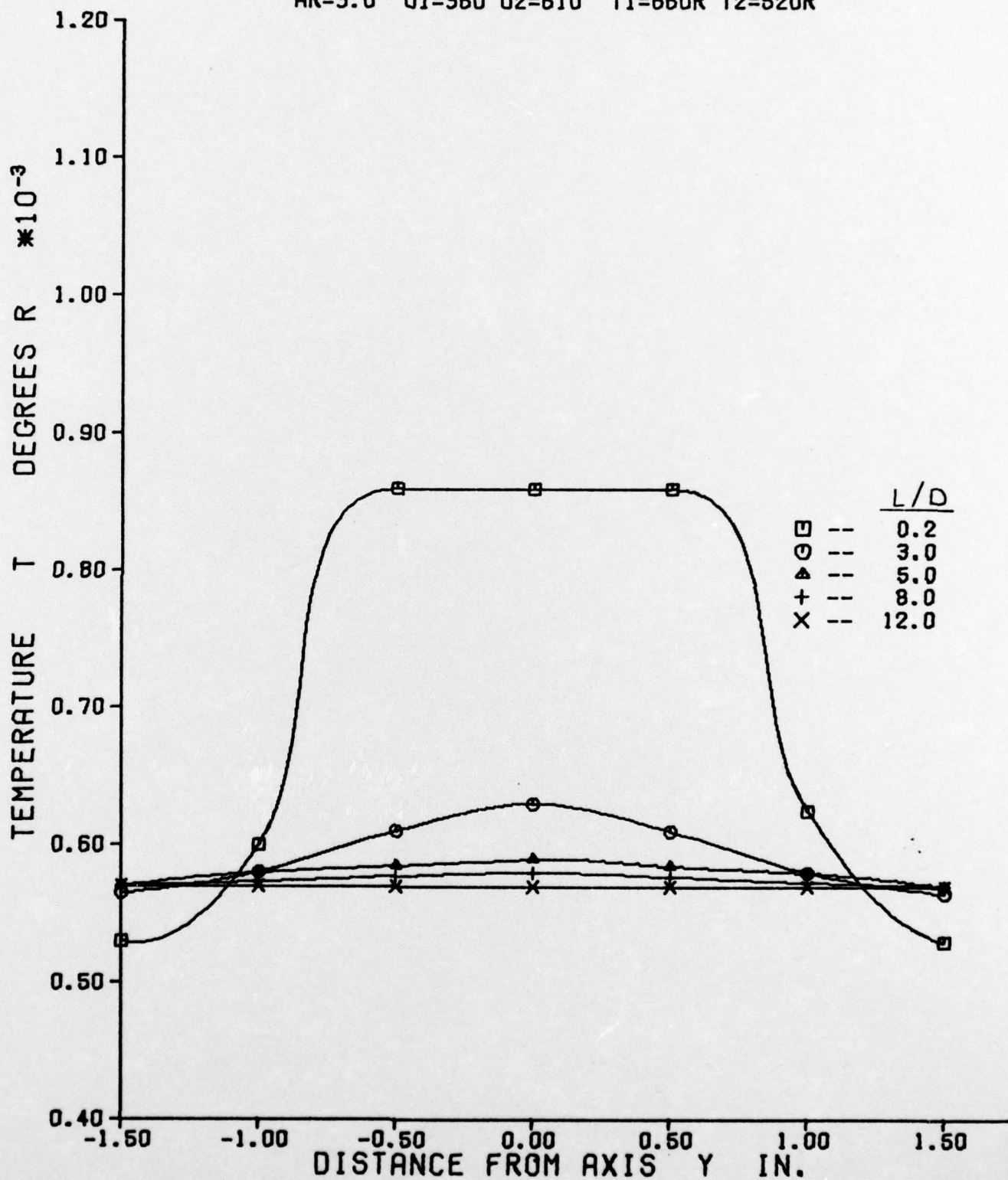AR=3.0 U1=360 U2=610 T1=860R T2=520R

FIGURE 8

EXPERIMENTAL TEMPERATURE PROFILES
AR=3.0 U1=770 U2=320 T1=960R T2=520R
e/R = 0.25

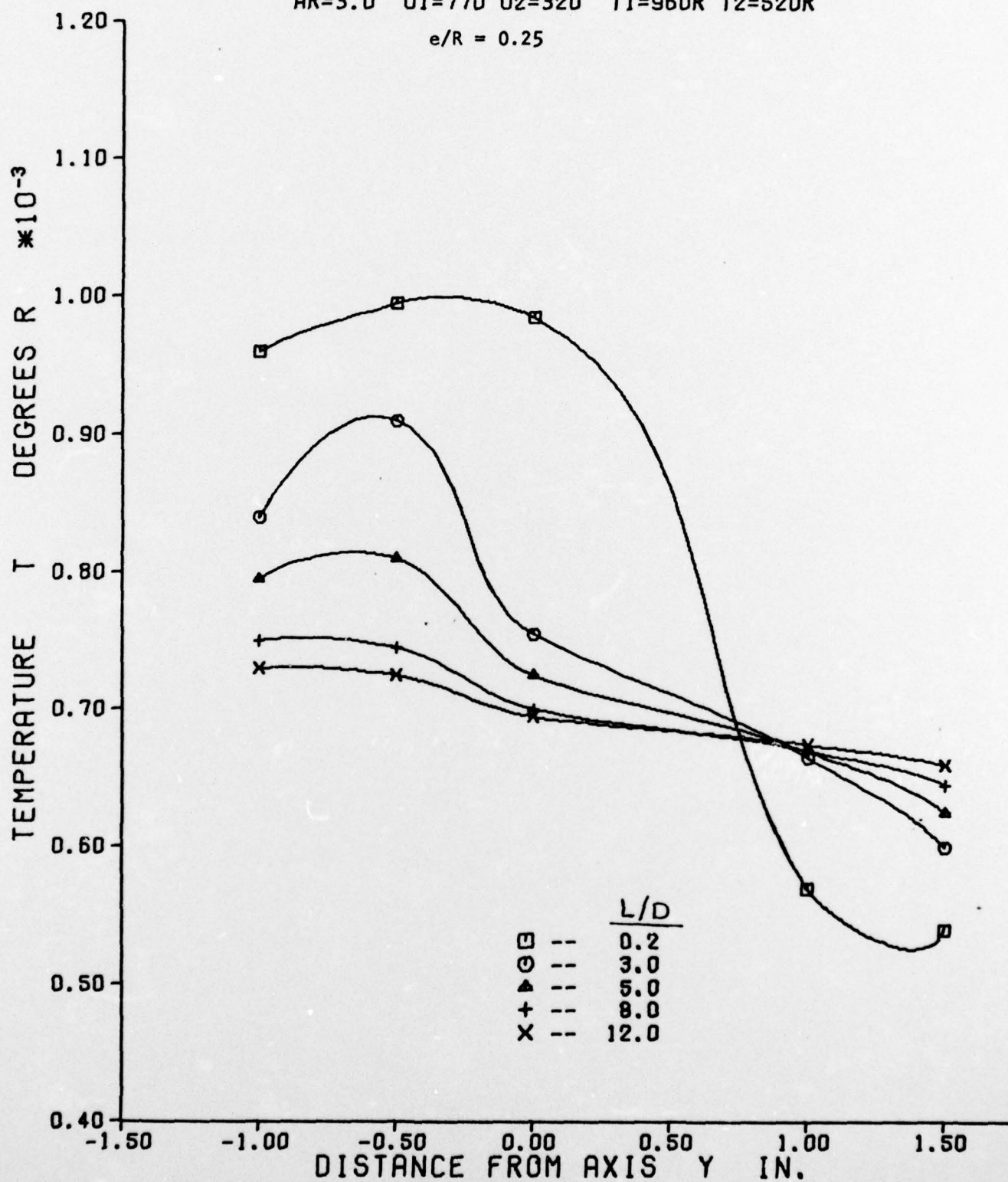FIGURE 9

EXPERIMENTAL TEMPERATURE PROFILES
AR=7.16 U1=860 U2=315 T1=960R T2=525R
e/R = 0.25
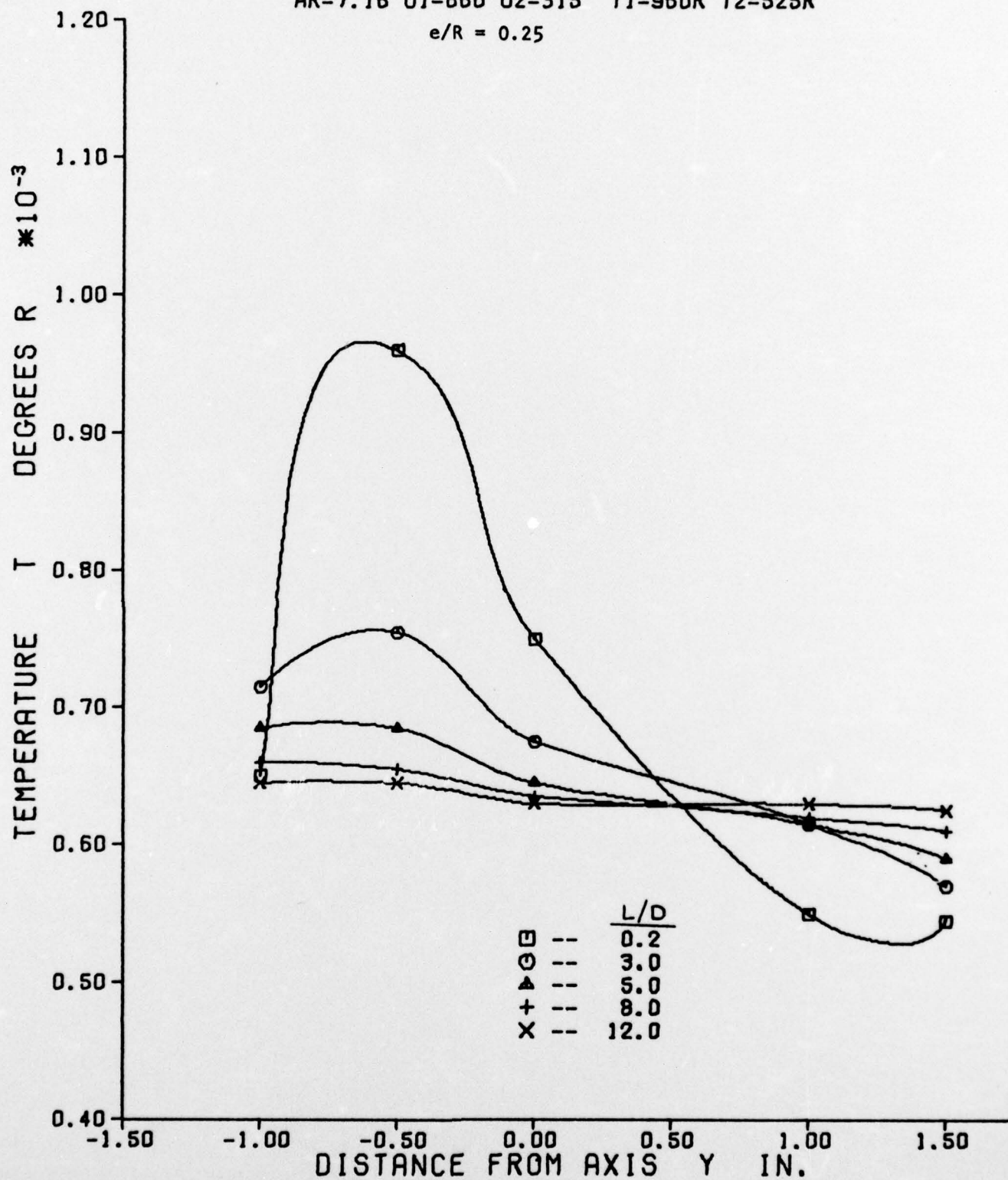
FIGURE 10

EXPERIMENTAL TEMPERATURE PROFILES
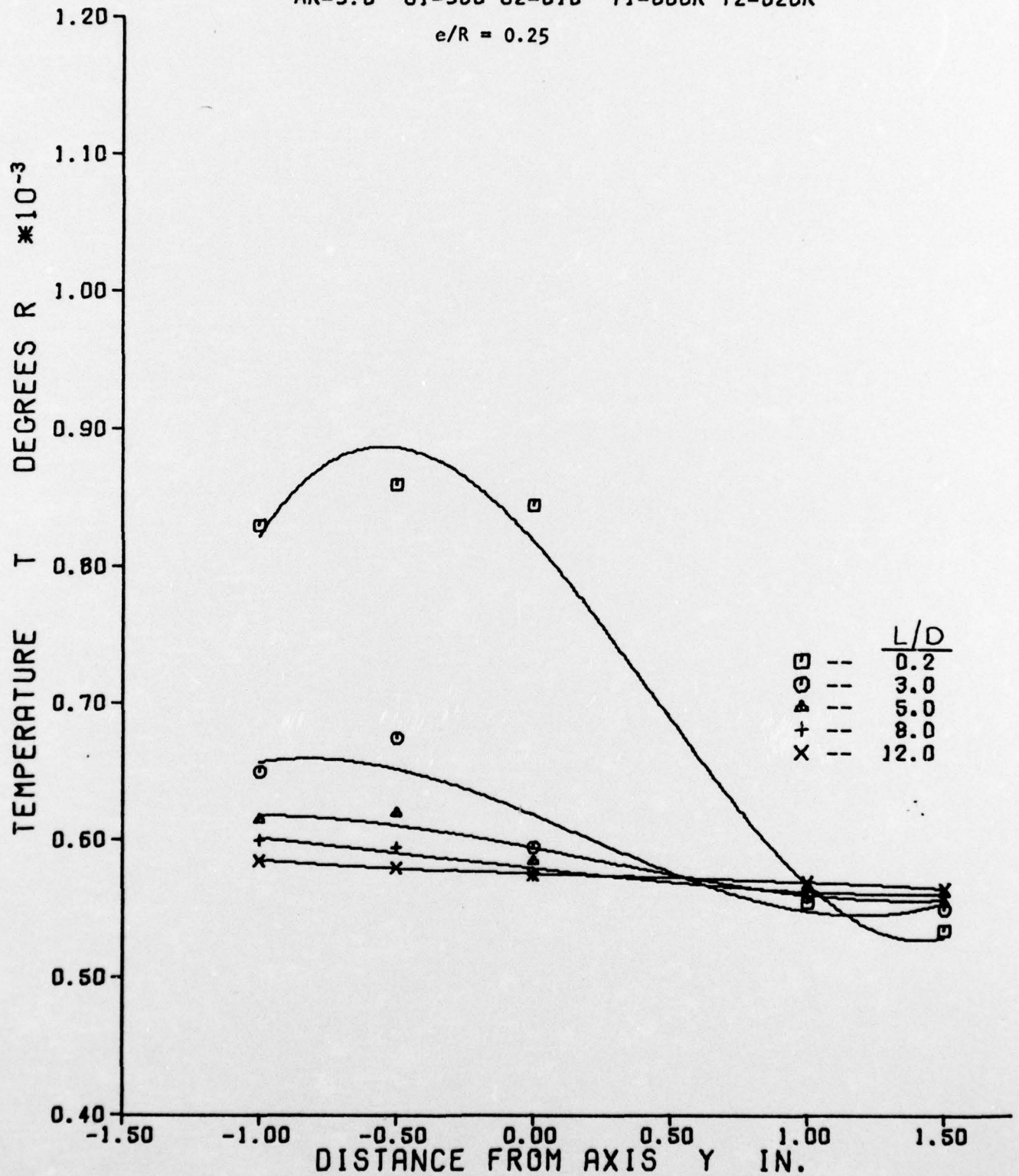AR=3.0 U1=360 U2=610 T1=860R T2=520R

e/R = 0.25

FIGURE 11

EXPERIMENTAL VS THEORETICAL TEMPERATURE COMPARISON
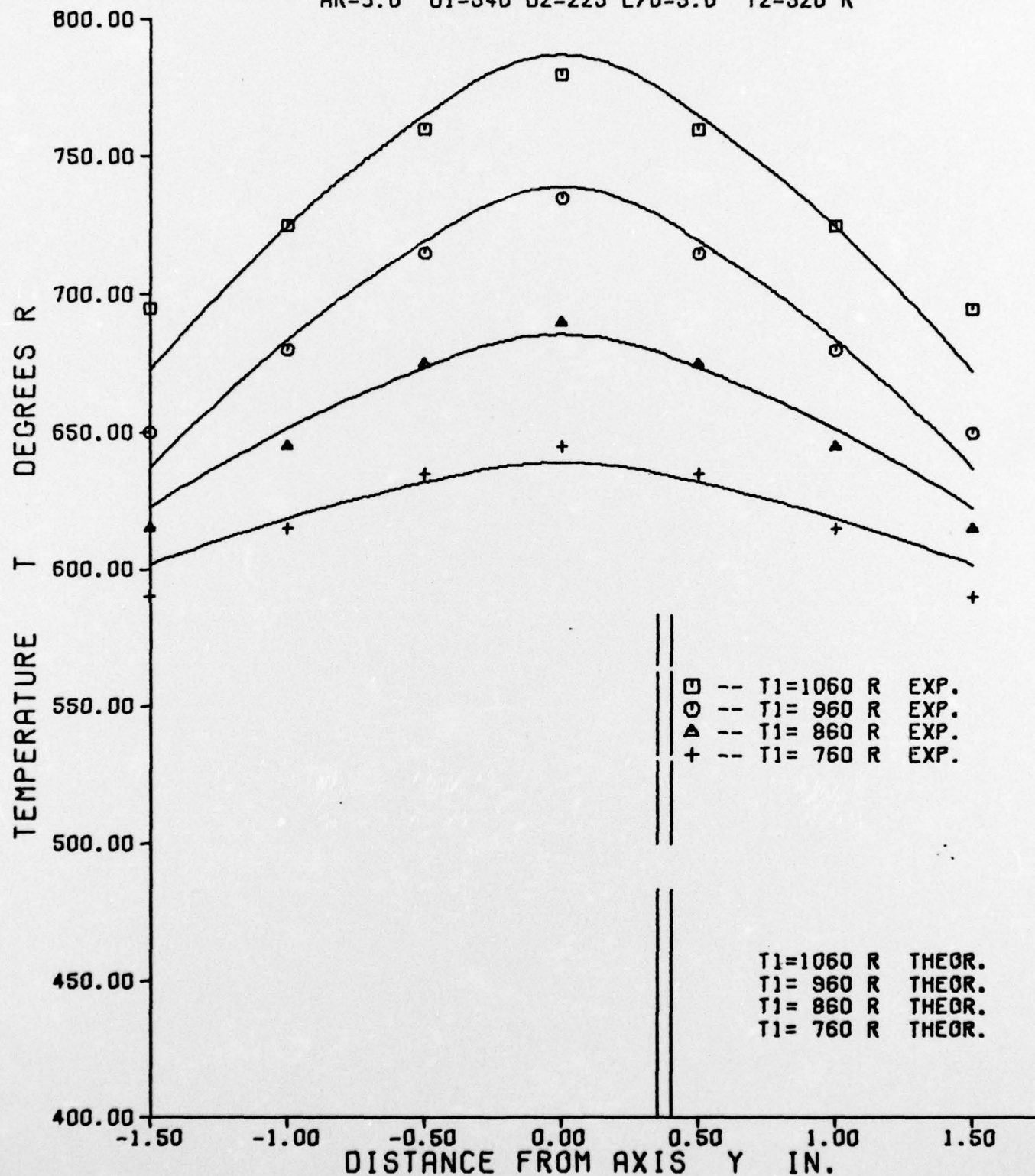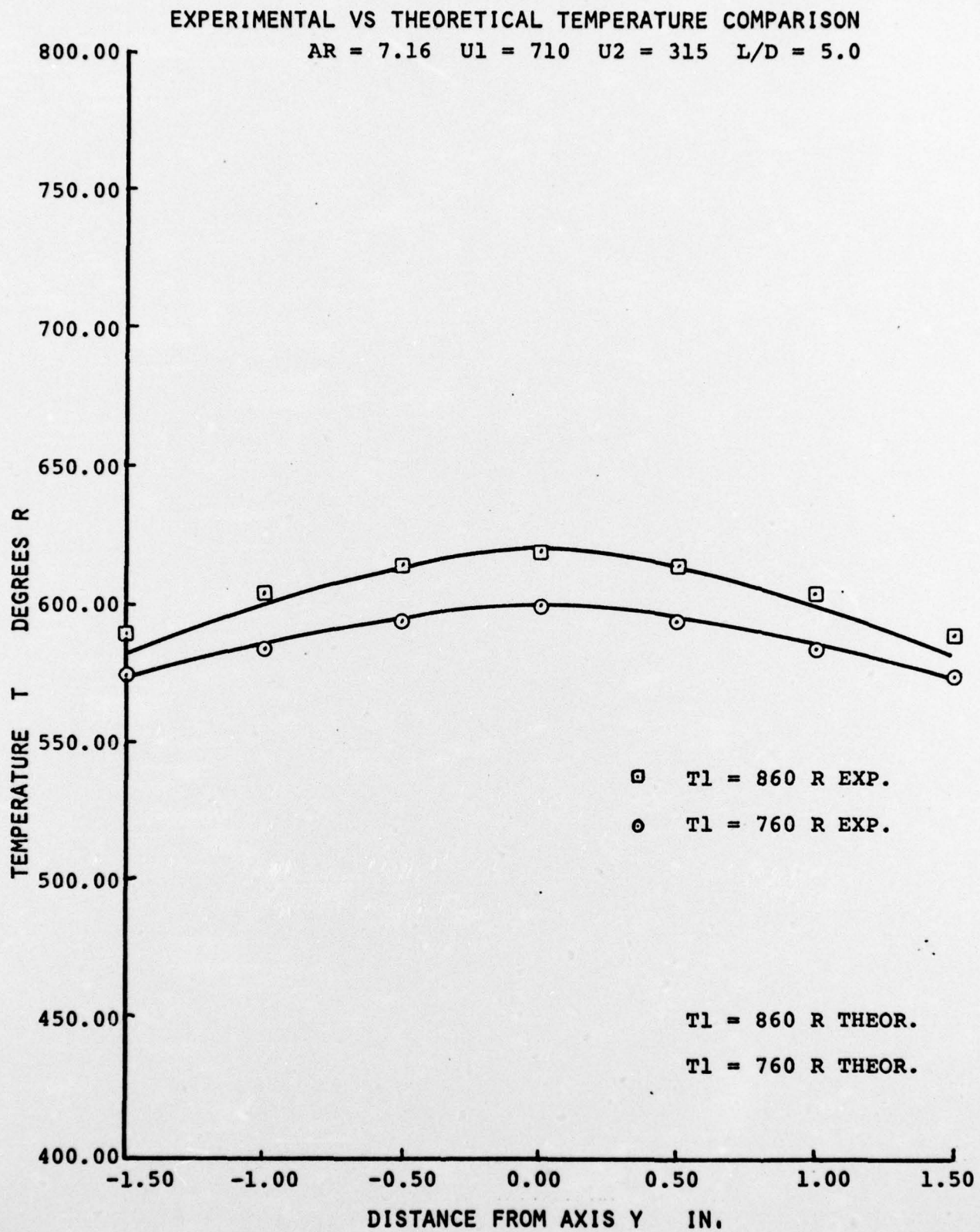AR=3.0   U1=540 U2=225 L/O=5.0   T2=520 R

FIGURE 13

EXPERIMENTAL VS THEORETICAL TEMPERATURE COMPARISON
AR = 7.16   U1 = 710   U2 = 315   L/D = 5.0

Tl = 860 R EXP.

Tl = 760 R EXP.

Tl = 860 R THEOR.

Tl = 760 R THEOR.

FIGURE 14

29

```fortran
C
      PROGRAM VELPLOT(INPUT,OUTPUT,TAPE5=INPUT)
CC    NON-ISOENERGETIC TURBULENT JET MIXING BETWEEN TWO STREAMS
CC    CENTRIC AND ECCENTRIC
CC    CONSTANT AREA DUCT
      DIMENSION VEL(45),T(45),DMLU(45),DRLT(10),URAT(10),TRAT(10)
    1 READ(5,10) T1X,T2Y,U1,U2,ARATIO
      READ(5,15) J,K,DEN,C,CH
   10 FORMAT(5F10.2)
   15 FORMAT(2I5,3F10.2)
   61 FORMAT (/2X3HU1=F8.2,2X3HU2=F8.2,2X3HU3=F8.2,2X3HUH=F8.2,2X3HT1=F8
     1.1,2X3HT2=F7.0,2X3HT3=F8.0,2X3HXN=F4.1,2X7HARATIO=F9.4,2X7HDEGOHT=
     2F7.3)
   62 FORMAT (3X7HTEMRAT=F12.5 ,4X5HPSYK=F7.3,4X5HLBAR=F9.2,4X7HDJFVEL=
     1F9.4,4X7HDJFTEM=F9.4,5X7HLNBAR=  F8.2)
   63 FORMAT (3X I3,5X5HPBAR=F7.2,5X2HU=F9.2,5X5HU/U3=F9.4,5X2HT=F9.1,1H
     1.,5X5HT/T3=F7.4,5X5HU/U1=F7.4,4X5HT/T1=F7.4)
      T2=T2Y+460.
      T1=T1X+460.
      DEGHOT=T1/T2
      XN=U2/U1*ARATIO*DEGHOT
      ALPHA=1./ARATIO
      THETA=1./DEGHOT
      T3=(T1+XN*T2)/(1.+XN)
      PRINT 60,C,CH
      ALPNTH=ALPHA*XN*THETA
      XM=ALPNTH*SQRT(1.-((2.*(1.-ALPHA*XN)*(1.-ALPNTH))/
     1(ALPNTH*XN*(ALPHA+1.)**2)))
      U3=U1*(1.+XN*THETA)*(ALPHA/(ALPHA+1.))
      UH=XM*U1
      PRINT 61,U1,U2,U3,UH,T1,T2,T3,XN,ARATIO,DEGHOT
      A=4.*XM/(1.-XM)
      XNBAR=1.5*(1.+XM)/(CH*(1.-XM)*SQRT(0.214+0.144*XM))
      RRYSR1=((ALPHA+1.)/ALPHA)**0.5
      XLNBAR= XNBAR/(2.*RRYSR1)
      KKK=0
      DO 25 LPSYK=J,K
      X1PSYK=LPSYK
      XPSYK=X1PSYK/DEN
      PSYK=1.-XPSYK
      A1PSYK=1.-1.143*((PSYK)**1.5)+0.4*((PSYK)**3)
      KKK=KKK+1
      IF (KKK-1) 31,31,18
   31 TEMRAT=DEGHOT
CC    TEMRAT=TH/T2
   18 TEMRAT=TEMRAT-0.005
      TEMP=TEMRAT/(TEMRAT-1.)
      BETA=TEMP**.333333
      SQPSYK=SQRT(PSYK)
      AA=ALOG((SQPSYK-BETA)**2/(SQPSYK**2+BETA*SQPSYK+BETA**2))
      Z=AA-3.4641*(ATAN2(2.*SQPSYK+BETA,1.732051*BETA))
      XPLFZR=SQPSYK+BETA*Z/6.+BETA*.3023
      P19A=(4.*(ALPHA*(XN*THETA+1.)-XM*(ALPHA+1.)))/(A1PSYK*
```

```
     1ALPHA*THETA*(XM+1.))
      P213=(SOPSYK**7/7.)+(((BETA**3-2.)/4.)*SOPSYK**4)+
     1((BETA**3-1.)**2)*XPLFZH
      P32C=4.*XM*(ALPHA+1.)*XPLFZR/(ALPHA*THETA*(XM+1.))
      P43D = SOPSYK**4/ (1. - TEMP)
      P54E = P10A*P21B + P32C
      P65F=ABS(P54E-P43D)
       IF (0.001 - P65F) 18,18, 20
   20 CONTINUE
      SMALA = TEMRAT - 1.
      A1 = .258*DEGGHT/ (1. + .626*SMALA)
      A2 = .134*DEGHT/ (1. + .745*SMALA)
      RCBAR = (8./(A2+XM*(2.*A1 -A2)))**0.5
      RNBAR = (1./(A2 +XM*(A1 -A2)))** 0.5
      RCMRNB =RCBAR - RNBAR
      XCMXNB =RCMRNB/((2.*C/A)*ALOG((2.+2.*A)/(2.+A)))
      RBYR1S = RBYSR1/PSYK
      BRCKT1 = ((RBYR1S - RNBAR)*(ALOG((2. + 2.*A)/(2. +A))))/RCMRNB
      BRCKT = EXP(BRCKT1)
      XSTAR = (((2. + A)*BRCKT - 2.)/A) - 1.
      XLBAR = (XNBAR + XSTAR*XCMXNB)/(2. * RBYSR1)
      TM = T2 * TEMRAT
      DELTM = TM - T2
      DELU3 = U3 - UH
      DELUM = DELU3/A1PSYK
      I = 0
      RBAR = 1.
   11 DELU = DELUM*((1. - (ABS(RBAR*PSYK))**1.5)**2)
      DELT = DELTM*(1. - (ABS(RBAR*PSYK))**1.5)
      I = I + 1
      VEL(I) = DELU + UH
      T(I) = DELT + T2
      DMLU(I) = VEL(I)/U3
      DMLT(I) = T(I)/T3
      URAT(I) = VEL(I)/U1
      TRAT(I) = T(I)/T1
      PRINT 63, I, RBAR, VEL(I), DMLU(I), T(I), DMLT(I), URAT(I), TRA
      RBAR = RBAR - 0.25
      IF (RBAR +1.01) 121, 11, 11
      IFVEL = (VEL(5) - VEL(1))/(U1 - U2)
      DIFTEM = (T(5) -T(1))/(T1 -T2)
      PRINT 62, TEMRAT,PSKY,XLBAR,DIFVEL,DIFTEM,XLNBAR
   25 CONTINUE
      GO TO 1
      END
```

DOCUMENT CONTROL DATA - R & D

(Security classification of title, body of abstract and indexing annotation must be entered when the overall report is classified)

1. ORIGINATING ACTIVITY (Corporate author)	2a. REPORT SECURITY CLASSIFICATION
University of Cincinnati	Unclassified
	2b. GROUP
	Na

3. REPORT TITLE

Study of Non-Isoenergetic Turbulent Jet Mixing in a Constant Area Duct

4. DESCRIPTIVE NOTES *(Type of report and inclusive dates)*

Technical Report

5. AUTHOR(S) *(First name, middle initial, last name)*

J.H. Blasenak and W. Tabakoff

6. REPORT DATE	7a. TOTAL NO. OF PAGES	7b. NO. OF REFS
September 1976	31	24

8a. CONTRACT OR GRANT NO.	9a. ORIGINATOR'S REPORT NUMBER(S)
DAHC04-69-C-0016	Report No. 76-49
b. PROJECT NO.	
c.	9b. OTHER REPORT NO(S) (Any other numbers that may be assigned this report)
d.	

10. DISTRIBUTION STATEMENT

Distribution of this report is unlimited.

11. SUPPLEMENTARY NOTES	12. SPONSORING MILITARY ACTIVITY
None	U.S. Army Research Office - Durham Box CM, Duke Station Durham, North Carolina

13. ABSTRACT

A study of non-isoenergetic turbulent jet mixing between two streams has been conducted. Using a previously derived theoretical analysis for ducted mixing, an experimental investigation was performed to verify this theory and to determine the non-isoenergetic turbulent jet mixing characteristics in a constant area duct. Temperature profiles were measured at several axial locations in the duct for both a concentric and an eccentric configuration. It was determined that the theoretical and experimental temperature profiles agreed fairly well for both cases, although the concentric case showed better agreement than the eccentric case. It was also determined that a new constant of turbulence in the initial region was needed for non-isoenergetic mixing, mixing is generally more rapid than the theory predicted, the initial temperature difference between the two streams did not have much effect on the rate of mixing and a higher area ratio produced better agreement between the theory and the experimental data. It was concluded that the theory was good for a fairly simplified analysis.

Key Words:

Gas Mixing

DD FORM 1473, 1 NOV 66 REPLACES DD FORM 1473, 1 JAN 64, WHICH IS OBSOLETE FOR ARMY USE.

Unclassified
Security Classification